PNNL-33296

Light Water Reactor Sustainability Program

Inverse Temperature Effects in Nuclear Power Plant Electrical Cable Insulation

September 2022

U.S. Department of Energy

Office of Nuclear Energy

PNNL-33296

Inverse Temperature Effects in Nuclear Power Plant Electrical Cable Insulation

Leonard S. Fifield, Yelin Ni, Donghui Li, Aishwarya Sriraman, Anthony Guzman, Angel Ortiz, Mychal P. Spencer, Mark K. Murphy, and Andy J. Zwoster

September 2022

Prepared for the
U.S. Department of Energy
Office of Nuclear Energy

SUMMARY

The Expanded Materials Degradation Assessment (EMDA) Volume 5: Aging of Cables and Cable Systems (NUREG/CR-7153, Vol. 5, 2014) relied on experts to assess aging and degradation of cabling and insulation in the context of potential second 20-year license renewals of operating nuclear power plants beyond their initial 60 years of operation. The EMDA identified several knowledge gaps that are areas of potential concern for the use of electrical cables beyond 60 years. One gap identified is related to the phenomenon that semi-crystalline insulation polymers may exhibit so-called inverse temperature effects when exposed to concurrent thermal and gamma radiation aging. In this scenario, degradation is found to proceed faster at lower temperatures than at higher temperatures. The concern is that pre-aging performed during cable qualification prior to accident survival assessment may not conservatively represent long-term aging in plant service. The EMDA recommended further "research to better understand inverse-temperature effects, identify which cable materials are most susceptible to these effects, and develop suitable methods to accelerate the aging of these materials." This report summarizes a portion of research conducted using the controlled thermal and gamma radiation application capabilities of the High Exposure Facility (HEF) at the Pacific Northwest National Laboratory to address this identified research need.

In this report, two electrical cable insulation materials most commonly used in containment in nuclear power plants considering second license renewal, Brand-Rex *Ultrol* cross-linked polyethylene (XLPE) and Samuel Moore *Dekoron* ethylene-propylene diene monomer (EPDM), were investigated to better understand inverse temperature effects in these materials. Insulation samples of these materials extracted from low voltage cables were exposed to a series of gamma radiation doses (up to 300 kGy) at constant dose rate (100 Gy/h) at three distinct temperatures (26, 50, and 90°C). As received and aged samples were characterized to quantify relative physical, chemical, and mechanical effects of the gamma aging at the three temperatures using the following metrics: tensile elongation at break (EAB), mass change, yellowness index, carbonyl index, density, and indenter modulus and relaxation constant.

The XLPE material investigated demonstrated evidence of inverse temperature effects in the tensile EAB results in which EAB decreased with dose faster at 26°C than at 90°C. EAB of XLPE fell below 50% of its unaged value at the lowest dose (50 kGy) at 26°C, whereas at 50°C and 90°C it did not approach 50% of initial value until 300 kGy. The EPDM insulation material considered proved to be quite robust to the accelerated aging conditions based on EAB performance, not falling below 50% of the initial performance by 300 kGy for any of the three temperatures. EAB for the 90°C exposed EPDM did not lose more than a third of its initial elasticity with the extreme 300 kGy explored. Interestingly, while XLPE exhibited detectable inverse temperature effects in its EAB performance, and EAB fell off abruptly with radiation dose at 26°C, degradation was found to track directly with temperature for every other physical quantity measured. That is, mass change, yellowness index, carbonyl index, indenter modulus, and relaxation constant values for XLPE were more different in the 90°C exposed samples than in the 50°C exposed samples, which were in turn more different than in the 26°C gamma exposed samples; such a trend was observed for all measurements for EPDM. Density was surprisingly not found to exhibit discernable trends with exposure in either material. The rapid loss of EAB performance at the 26°C exposure for the XLPE considered is potentially concerning regarding assumptions made in extrapolation of accelerated aging to service lifetime, but the other characteristics measured for this material are consistent with an Arrhenius-based estimation of degradation with temperature for this material and the EPDM considered.

The results in this report do not support the conclusion that ITE in cable qualification necessarily exclude safe continued use of existing cables. Inverse temperature effects were found to differ based on insulation material and on property measured. The practice of subjecting cables to thermal aging followed by radiation aging at room temperature in qualification appears to be a conservative scenario for materials exhibiting ITE. Ongoing non-destructive cable system condition monitoring is encouraged to support repair and replace decisions for continued safe and effective use of electrical cables in long term operation.

ACKNOWLEDGEMENTS

This work was sponsored by the U.S. Department of Energy, Office of Nuclear Energy, for the Light Water Reactor Sustainability (LWRS) Program Materials Research Pathway. The authors extend their appreciation to Pathway Lead Dr. Thomas Rosseel for LWRS programmatic support. This work was performed at the Pacific Northwest National Laboratory (PNNL). PNNL is operated by Battelle for the U.S. Department of Energy under contract DE-AC05-76RL01830.

CONTENTS

FIGURES

TABLES

ACRONYMS

ASTM	ASTM International
ATR	attenuated total reflectance
CI	carbonyl index
CIE	International Commission on Illumination
CFR	Code of Federal Regulations
CPE	chlorinated polyethylene
CSPE	chlorosulfonated polyethylene
DLO	diffusion limited oxidation
DOE	Department of Energy
EAB	elongation at break
EMDA	Expanded Materials Degradation Assessment
EPDM	ethylene-propylene-diene elastomer
EPR	ethylene-propylene rubber
EPRI	Electric Power Research Institute
HEF	High Exposure Facility (at PNNL)
IEC	International Electrotechnical Commission
IEEE	Institute of Electrical and Electronics Engineers
IM	indenter modulus
IPAM	Indenter Polymer Aging Monitor
ISO	International Organization for Standardization
ITE	inverse temperature effects
LOCA	loss-of-coolant accident
NIH	National Institute of Health
NPP	nuclear power plant
NRC	Nuclear Regulatory Commission
PE	polyethylene
PNNL	Pacific Northwest National Laboratory
SLR	subsequent license renewal
XLPE	cross-linked polyethylene
XLPO	cross-linked polyolefin
YI	yellowness index

1. INTRODUCTION

Approximately 20% of the electricity produced in the United States comes from nuclear power plants (NPPs) (EIA, 2022). Originally, NPPs were qualified for an operational lifetime of 40 years (Gazdzinski et al., 2000; Subudhi, 1996). As described in the foreword of the U.S. Nuclear Regulatory Commission's (NRC's) Expanded Materials Degradation Assessment (EMDA) Volume 5: Aging of Cables and Cable Systems (NRC, 2014), and according to Title 10 of the Code of Federal Regulations, Part 54 (10 CFR 54), Requirements for Renewal of Operating Licenses for Nuclear Power Plants, NPPs can apply for 20-year license extensions following the original 40-year operating period. While most NPPs have entered extended license periods to 60 years, some are considering license extension to 80 years of operation. The viability of a subsequent license renewal (SLR) is dependent upon the NPP operating safely in accordance with the licensing basis established with the original 40-year license. Hence, the NRC has developed aging management program requirements to ensure the safe operation of NPPs over license extension periods. The EMDA report identified cable aging-related issues that may be important for the SLR of NPPs.

Based on the issues raised in EMDA Volume 5, a U.S. Department of Energy-sponsored research and development roadmap workshop report (Simmons et al., 2012), and additional emerging issues, Pacific Northwest National Laboratory (PNNL) prioritized a list of 11 cable-aging knowledge gaps focusing on the degradation of cable insulation (Fifield et al., 2018). From this list, four knowledge gaps were selected for investigation as described by Fifield et al., including: (1) inverse temperature effects (ITE) in which degradation due to gamma irradiation is higher at lower temperatures (Przybytniak et al., 2015), (2) diffusion limited oxidation (DLO) effects due to oxygen permeability hindrance at the polymer surface during accelerated aging (Gillen and Clough, 1992), (3) dose-rate effects where polymer degradation is not only a function of total absorbed gamma dose, but also of the dose rate (Gillen and Clough, 1989), and (4) synergistic effects due to the combined interactions between temperature and radiation (Gillen, 2019; Seguchi et al., 2011). The inverse temperature effects phenomenon is the focus of this report.

Historically, manufacturers qualified electrical cables for 40-year operational lifetimes using accelerated aging at temperatures and gamma radiation dose rates well above those experienced by cables in service (Seguchi et al., 2015). Previous work identified situations where polymeric NPP cable insulation degrades faster at lower temperatures under gamma irradiation than at higher temperatures, referred to as inverse temperature effects or ITE (Celina et al., 1996). ITE have only been observed in semi-crystalline polymers, such as cross-linked polyethylene, undergoing combined or simultaneous thermal and gamma irradiation. Accelerated combined thermal and gamma irradiation aging to predict cable performance and lifetime under milder, long-term conditions may underestimate degradation if ITE were present. Uncertainties still exist regarding the impact of ITE, such as which metrics are sensitive to ITE and the effect of ITE on NPP electrical cable lifetime. To support SLR of NPPs to 80-years or more, additional information regarding the impact of ITE on the historical qualification of electrical cables is needed.

In this study, common nuclear cable insulation materials (Subudhi, 1996)—cross-linked polyethylene (XLPE) and ethylene propylene diene elastomer (EPDM)—were aged at three temperatures (26°C, 50°C, and 90°C) with constant cobalt-60 gamma-ray dose rate for select exposure durations to evaluate ITE. First, in Section 2, the cable insulation material types investigated are described. Then, in Section 3, accelerated aging involving elevated temperature and gamma irradiation applied to the insulation specimens is discussed. In Section 4, the characterization techniques used to perform this work are described. These include elongation at break (EAB), mass change, yellowness index (YI), carbonyl index (CI), density, indenter modulus (IM), and relaxation constant. Section 5 discusses the theory of polymer degradation. Characterization results and discussion are provided in Section 6 and Section 7, respectively. Finally, concluding remarks are made in Section 8.

2. MATERIALS

The materials investigated were selected from those commonly found within nuclear containment to enhance the relevancy of this work. Both XLPE and EPDM were selected for analysis of ITE effects because insulation material types like these are present within at least 75% of nuclear containments in U.S. NPPs, as shown in Table 1. In addition to the targeted material types, low-voltage nuclear grade instrumentation cables were selected because approximately 81% of electrical cables within U.S. NPPs are low-voltage instrument and control cables (Gazdzinski et al., 1996). Furthermore, the investigated materials were extracted from cables produced by two of the most commonly utilized manufactures of electrical cables for NPPs as shown in Table 1 and Table 2. One of the as-received electrical cables of this report was harvested from the decommissioned Crystal River Unit 3, an activity coordinated by the Electric Power Research Institute (EPRI) (Fifield, 2016; Fifield et al., 2016). As such, this material has previous aging history that is not accounted for in the analyses of this report (see Table 3).

Table 1. Most common nuclear cable insulation material types in containment (left) and a sort of the most common manufacturers' insulations within NPPs (right). (Percent of units indicated are approximate values.)

Insulation	**Percent of Units (%)** (Gazdzinski et al., 1996)
XLPE	90
EPDM/EPR	75
SR	27
CSPE	24
ETFE	15
PVC	7
PE	3
Neoprene	3
Polyimide	3
Polyalkene	2

Manufacturer	**Insulation**	**Number of Plants** (Gazdzinski et al., 1996)
Rockbestos	Firewall III XLPE	61
Anaconda	EPR	35
Brand-Rex	XLPE	30
Okonite	EPR	26
Kerite	HTK	25
Rockbestos	Coaxial XLPE	24
Raychem	XLPE	23
Samuel Moore	EPR	19
BIW	Bostrad 7E EPR	19
Kerite	FR EPR	13

XLPE = cross-linked polyethylene; EPDM = ethylene-propylene-diene elastomer; EPR = ethylene-propylene rubber and ethylene-propylene diene monomer (EPDM); SR = silicone rubber; CSPE = chlorosulfonated polyethylene; ETFE = ethylene tetrafluoroethylene; PVC = polyvinyl chloride; PE = polyethylene; HTK = high-temperature Kerite; FR = flame retardant.

Table 2. Nuclear grade instrumentation cables used in this report.

Identifier	**Manufacturer**	**Jacket Labeling**	**Jacket Material**	**Insulation Material**
XLPE	Brand-Rex	Ultrol 600V Shielded PR #16 AWG	CSPE	XLPE
EPDM	Samuel Moore	Dekoron 2/C 16 AWG 600V	CSPE	EPDM/EPR

XLPE = cross-linked polyethylene; EPDM = ethylene-propylene-diene elastomer; EPR = ethylene-propylene rubber; CSPE = chlorosulfonated polyethylene; CPE = chlorinated polyethylene.

Table 3. Aging history of the electrical cables of this report.

Identifier	**Manufacture Date**	**Installation Date**	**Location**	**Years in Service**
XLPE	1986	1994, Crystal River Unit 3	Main Feedwater	21
EPDM	No previous aging history			

2.1 Components of As-Received Electrical Cables

Components of the low-voltage nuclear grade instrumentation cables of this report are shown in Figure 1. The white insulated conductors were extracted from the electrical instrumentation cables of Table 2 by first carefully removing the chlorosulfonated polyethylene (CSPE) jackets. A wire stripping tool was then used to score the insulation in 100 mm increments. Afterwards, the exposed conductors were fixed in place with a vice and the insulation removed by gently pulling the insulation from over the conductors. The extracted insulation specimens were 100 mm in length. The tubular cross-sections of the insulation specimens were measured as 4.80 mm^2 (2.81 mm outer diameter) and 4.64 mm^2 (2.78 mm outer diameter) for the XLPE and EPDM insulations, respectively.

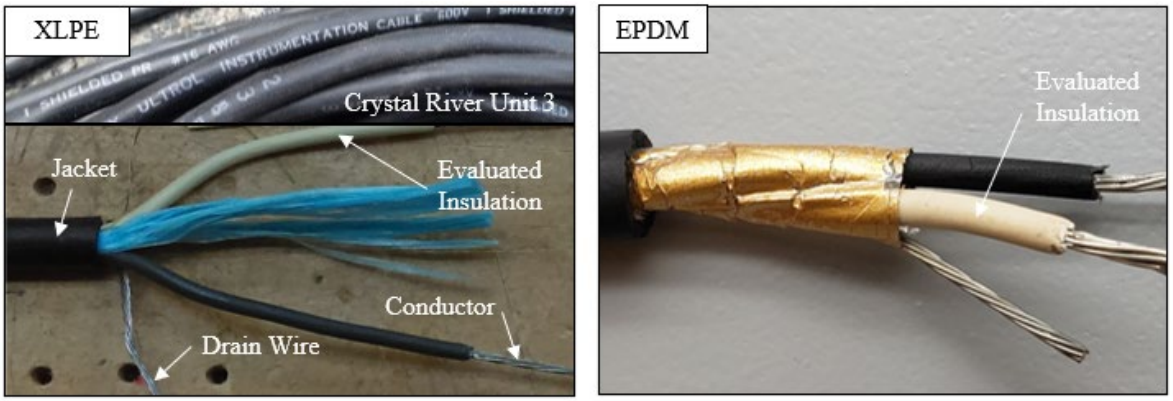

Figure 1. The as-received nuclear grade electrical cables and their exposed components. The evaluated white insulations selected for analysis are indicated in the figure.

3. THERMAL AND RADIATION AGING

Insulation specimens were attached to clips labeled with unique specimen identifiers. The specimens were hung from a rack in an oven (Quincy Lab, Inc. 10AF) and exposed to one of the conditions shown in Table 4. To evaluate the effects of ITE, dose rate and total dose were held constant for each aging condition. Using an approximately 11,000 Ci cobalt-60 (Co-60) source, gamma irradiation was conducted at the High Exposure Facility (HEF) at PNNL. A dose rate of approximately 100 Gy/hr was obtained by positioning the specimens at approximately 88 cm from the Co-60 source. Temperature was controlled through integrated thermocouple feedback and the oven was modified to enable the heating elements to be independent of the oven fans to maintain air circulation in the absence of heating. With no heating, the oven was at an ambient temperature of 26°C. Unaged specimens were evaluated for benchmark reference.

Table 4. Evaluated test conditions for exposure of nuclear grade cable insulation specimens.

T (°C)	Target Total Dose (kGy)	T (°C)	Target Total Dose (kGy)	T (°C)	Target Total Dose (kGy)
26	50	50	50	90	50
26	90	50	90	90	90
26	130	50	130	90	130
26	170	50	170	90	170
26	210	50	210	90	210
26	250	50	250	90	250
26	300	50	300	90	300

4. EXPERIMENTAL METHODS

To investigate ITE for the selected materials, six characterization methods were employed as discussed below.

4.1 Elongation at Break Measurement Using a Tensile Machine

Following IEC/IEEE 62582-3, tensile EAB was measured for as received and aged insulation specimens. For each aging condition, the insulation specimens were cut to a length of 50 mm and the inner and outer diameters were measured using a digital caliper. Afterwards, the insulation specimens were conditioned following ASTM D618 Procedure A: at least 40 hours at 23°C ± 2°C and 50% ± 10% relative humidity. Humidity was controlled by placing the specimens within an environmental chamber (Caron Model 7000-25).

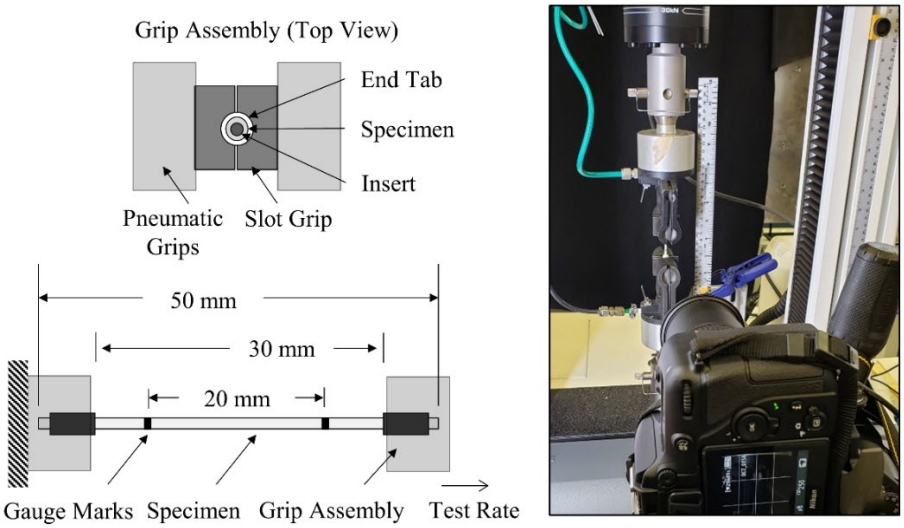

Figure 2. (Left) testing schematic for tensile testing of the insulation specimens and (right) digital image of the test frame.

After conditioning, a black permanent marker with a fine tip size was used to draw two gauge marks centered and at 20 mm separation on the insulation specimens. End tabs of 10 mm length (polyvinyl chloride) were then placed over the ends of specimens with an approximate gap of 1 mm between the ends of specimens and the end tabs (see Figure 2). In addition, inserts (low density polyethylene) of length 10 mm were placed within the insulation at both ends. After attachment of the end tabs and inserts, the grip assembly varied based upon material type and irradiation temperature. Specifically, XLPE specimens aged at 26°C were placed within a custom-made slot grip (see Figure 2 for more details) to reduce early failure of these specimens. All other specimens were directly clamped within a pair of pneumatic grips at 40 psi and at a separation of 30 mm. As shown in Figure 2, a tensile testing machine (Instron® 3360 Universal Testing System, Norwood, MA) was used to apply tension to the specimens. A test rate of 10 mm/min and 20 mm/min was selected for XLPE and EPDM specimens, respectively. A testing rate lower than that specified in IEC/IEEE 62582-3 was used to minimize early failure of specimens. Elongation at break was estimated for each specimen using captured videos of the specimen deformation; the gauge length was evaluated in ImageJ (NIH) prior to force loading and just prior to failure and EAB was calculated as the difference between the final and initial gauge length divided by the initial gauge length. For each aging condition, EAB was calculated for three insulation specimens and the average value reported. Samples that experienced premature failure (e.g., as observed by failure in the grip before tension was applied) were removed from the data sets, resulting in some specimens having fewer corresponding data points.

4.2 Mass Change Measurement Using an Analytical Balance

An analytical balance (Fisher Scientific ALF104, ± 0.001 g resolution) was used to measure the mass of the insulation specimens before and after aging. The mass of three insulation specimens was measured for each aging condition.

4.3 Yellowness Index Measurement Using a Digital Camera

Polymeric specimens darken upon aging when exposed to thermal stress. Following ASTM D1729 and ASTM D2244, yellowness index (YI) of the aged with respect to the as-received insulation specimens was measured using a light booth (GTI MiniMatcher MM 2e) and a digital camera (Nikon D7500). A clamp was used to fix the digital camera in place and orient the camera lens perpendicular to the display plane of the light booth. To optimize the quality of the collected images, the digital camera settings used were as follows: an exposure time of 1/20 s to enhance color saturation, an aperture of f/5 to enhance depth of field, and an ISO setting of 100 to reduce background noise. A wireless remote control (Nikon ML-L3) was used to ensure the camera did not move during image collection and to facilitate batch processing. In the light booth, a standard International Commission on Illumination (CIE) D65 light was used and background lighting in the room was extinguished during image collection. To facilitate image calibration and conversion to the CIE XYZ color space, a color reference target was placed on the light booth display plane next to the specimen. Because of issues with surface reflections on tubular specimens and variations in color along the specimen lengths, each insulation specimen was removed after image collection, rotated slightly, and then returned next to the color reference target before another image was captured. This process was repeated twice for a total of three images per insulation specimen.

Due to their inherent components and internal processing, a digital camera and lens will modify the color in digital images; therefore, it is necessary to map these modified colors into a system with an absolute measure of color prior to quantifying color changes in specimens tested. ImageJ (NIH) was used in conjunction with the micaToolbox (Troscianko, 2020; Troscianko and Stevens, 2015) to convert the collected image values to CIE XYZ color space. First, the six grey standards located on the bottom row of the color reference target were converted to reflectance values using manufacturer-supplied standard Red Green Blue (sRGB) triplets for each grey standard and then using an iterative least log slope approach (Burns, 2017) to convert the triplets to reflectance values. Second, the grey reflectance values were used to create a linear normalized reflectance stack, or calibrated multispectral image, for each collected image. Third, a cone-catch model (Troscianko and Stevens, 2015) was generated based upon the charted reflectance spectra of the color reference target. Lastly, the cone-catch model was used to map the linear normalized reflectance stack to the CIE XYZ color space. Calculation of yellowness index for a D65 illuminant is shown in Equation (1), where X, Y, and Z are the evaluated XYZ tristimulus values of the specimen.

$$YI = 100\,(1.2985 \cdot X - 1.1335 \cdot Z)/Y \tag{1}$$

4.4 Carbonyl Index Measurement using FTIR

Fourier-transform infrared spectroscopy (FTIR) may be used to identify chemical changes in materials through the tracking of absorption intensities at characteristic absorbance energies. This technique enables determination of the carbonyl index (CI), which is a measure of the conversion of C-C or C-H bonds to carbonyl (C═O) bonds due to oxidation. In this work, CI was measured to track oxidation occurring as a result of the aging process.

Carbonyl index measurement was conducted using an FTIR (Bruker Alpha II) equipped with an attenuated total reflection (ATR) attachment. A 10 mm-long sample was extracted from the end of each

insulation specimen prior to FTIR measurement. The extracted samples were pre-conditioned in a controlled environment of 23°C ± 2°C and 50% ± 10% relative humidity for at least 40 hours. Humidity was controlled by placing the samples within an environmental chamber (Caron Model 7000-25). Following conditioning, individual samples were centered on a diamond ATR crystal. For each sample, 64 scans were collected at a resolution at 4 cm^{-1} to minimize signal variation due to random noise. Three replicate measurements were taken per sample. After measurement, analysis of the collected FTIR spectra was performed using the hyperSpec package in R (Beleites and Sergo, 2013). Carbonyl index (CI) was determined as the ratio between the band absorbance intensity of the carbonyl peak (at 1715 cm^{-1}) ($A_{C=O}$) and that of the methylene symmetric stretch peak (between 2846 and 2850 cm^{-1}) (A_{C-H}) as shown below in Equation (2).

$$CI = A_{C=O}/A_{C-H} \tag{2}$$

4.5 Density Measurement using Archimedes' Principle

Following ASTM D792, the density of the insulation specimens was measured. An approximate length of 5 mm was extracted from the end of the insulation specimens for density measurement. The extracted samples were pre-conditioned in a controlled environment of 23°C ± 2°C and 50% ± 10% relative humidity for at least 40 hours. Humidity was controlled by placing the samples within an environmental chamber (Caron Model 7000-25). A high-resolution analytical balance (Mettler Toledo™ XPR205, ±0.00005 g) was used in conjunction with a density measurement kit (Mettler Toledo™ Density Kit, XPR/XSR-Analytical 30460852) to measure sample mass in air and in water. Prior to immersing a sample, the mass in air was measured. Afterwards, the sample was wetted with isopropanol alcohol to limit formation of air bubbles on the sample surface. Each sample was then immediately placed in a convex sample holder immersed in deionized water (24.6°C ± 0.9°C); the sample holder was located at a depth of approximately 2.5 cm below the surface. The sample apparent mass was then recorded and the sample was removed, again wetted with isopropanol, and set aside to dry. The above process was repeated two times for a total of three sets of measurements per insulation specimen (a total of three measurements for each aging condition). The Archimedes' principle (water displacement) was used to determine the density (g/cm^3) as shown in Equation (3), where m is the average mass in air (g), m_l is the average mass immersed in water (g), and ρ_l is the density of the liquid (g/cm^3) at the measurement temperature.

$$\rho = m\rho_l/(m - m_l) \tag{3}$$

4.6 Indenter Modulus and Relaxation Constant Measurement

The indenter modulus (IM) of the insulation specimens was measured following IEC/IEEE 62582-2. Specimens were pre-conditioned in a controlled environment of 23°C ± 2°C and 50% ± 10% relative humidity for at least 40 hours. Humidity was controlled by placing the samples within an environmental chamber (Caron Model 7000-25). After conditioning, insulation specimens were placed within a cable clamp assembly of an Indenter Polymer Aging Monitor (AMS Corp. IPAM 4M, Tennessee, USA). The insulation specimens were then gently clamped within the IPAM to prevent displacement during measurement. An instrumented probe housed within the IPAM indented the external surface of the specimens at a displacement rate of 5.1 mm/min to a maximum load of 8.9 N, similar to the recommendations of IEC/IEEE 62582-2. Each measurement was conducted under ambient laboratory conditions (approximately 21°C and 30% relative humidity). The indentation process was controlled, and data collected, through the usage of an external pocket PC. For each insulation specimen, a total of ten indentations were performed at three locations around the specimen circumference while avoiding indentation within 10 mm of each end of the specimen. Per IEC/IEEE 62582-2, the indenter modulus (N/mm) was calculated from the slope of the linear portion of the initial force versus deformation curve as shown in Equation (4), where d_1 and d_2 are the displacements (mm) corresponding to force values of F_1 (1

N) and F_2 (4 N), respectively. In addition to the indenter modulus, the IPAM allows for easy measurement of the insulation specimen relaxation constant, τ. After the maximum load (8.9 N) has been reached during indentation, the probe stops moving and relaxation of the polymeric insulation was measured over time. The relaxation constant (s) is shown in Equation (5), where F_3 and F_4 are the force (N) values corresponding to measurement times of t_3 (2 s) and t_4 (3 s) after the probe has stopped moving, respectively. The average value and standard deviation of the indenter modulus and relaxation constant were reported after removing the highest and lowest measurement values due to variation in specimen construction, dimensions, and stabilization.

$$IM = (F_2 - F_1)/(d_2 - d_1) \quad (4)$$

$$\tau = |(t_4 - t_3)/ln(F_4/F_3)| \quad (5)$$

5. POLYMER DEGRADATION THEORY

Polymers have become ubiquitous in modern NPP infrastructure. As such, their response to the harsh environments of NPPs has attracted significant interest and been the subject of many studies. There are three primary modes of chemical degradation of polymers in an NPP environment: thermal, radiative, and oxidative. Whenever thermal or radiative degradation occurs in an oxygenated environment these mechanisms become known as thermal-oxidation or photo-oxidation, and oxidative reactions dominate the degradative reaction pathways (Zhang et al., 2020).

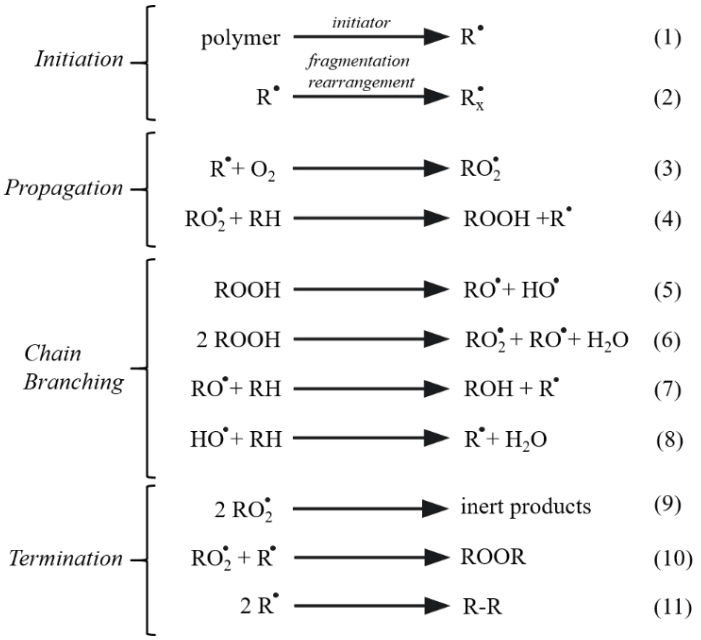

Scheme 1. Basic auto-oxidation scheme (Gryn'ova et al., 2011).

Most polymers are thought to undergo oxidative degradation under normal conditions by an autocatalytic process known as auto-oxidation. J. L. Bolland first established the modern understanding of the mechanism of polymer auto-oxidation (Gryn'ova et al., 2011). The process is described in several steps including initiation, chain propagation, chain branching, and termination, as shown in Scheme 1. Initiation (Scheme 1, (1)) occurs as weak C-H bonds break, leading to the formation of free radicals (R·). These free radicals can then rearrange (Scheme 1 (2)) without terminating the degradation reaction. Regardless, generated radicals quickly react with oxygen to form peroxyl radicals (RO_2·), which quickly stabilize into hydro-peroxides (ROOH) through propagation reactions (Scheme 1 (3, 4)). Generated hydro-peroxides can

then decompose to form RO· and HO·, which results in chain branching reactions (Scheme 1 (5-8)). Ultimately, however, generated radicals form inactive products like carbonyl groups or unsaturated groups through termination reactions (Scheme 1 (9-11)).

6. RESULTS

A concern has been raised that ITE could lead to overestimation of the predicted useful life of certain semi-crystalline polymeric NPP cable insulation. A variety of characterization techniques were employed to assess ITE and to supply more complete information to regulators, operators, and other decision-makers about the long-term operation of nuclear electrical cables exhibiting ITE. All measurements were compared to the as-received specimens to avoid issues with aging history.

6.1 Elongation at Break

Evaluation of EAB with respect to the unaged specimens is shown in Figure 3. For both material types, a roughly sigmoidal shape was observed, similar to previous work (Fifield et al., 2020). As shown, ITE was observed with XLPE only. More specifically, EAB was not found to decay below 50% relative EAB at irradiation temperatures of 50°C or 90°C for all doses explored for XLPE and for all doses and temperatures explored for EPDM; however, an approximately 0% relative EAB, indicating total degradation of the material, was observed at an irradiation temperature of 26°C at approximately 200 kGy for XLPE. Previous work has identified such an inverse temperature response to be associated with ITE (Celina et al., 1998). Although a slightly reduced rate of degradation with dose was observed at the higher temperatures for EPDM, degradation behavior was similar for all three temperatures and EAB only approached 50% of the initial value at the highest dose of 300 kGy. Regarding the effect of temperature on relative EAB of EPDM, the three isotherms showed similar trend with the increase of dose, which cannot be fit by Arrhenius model or be explained by ITE. At the investigated aging conditions, EPDM was subjected to radiation-dominant degradation.

Although 50% absolute elongation at break for insulation is often used as a generic definition of cable end of life, as defined by ability to pass a loss-of-coolant accident (LOCA) simulation, some cables have been observed to pass a LOCA test at much lower EAB (e.g., 10%). Furthermore, EAB has not always used by cable manufacturers to define their pass/fail criteria for cable accelerating aging in qualification. For other metrics, such as dielectric breakdown, the presence or impact of ITE is unclear.

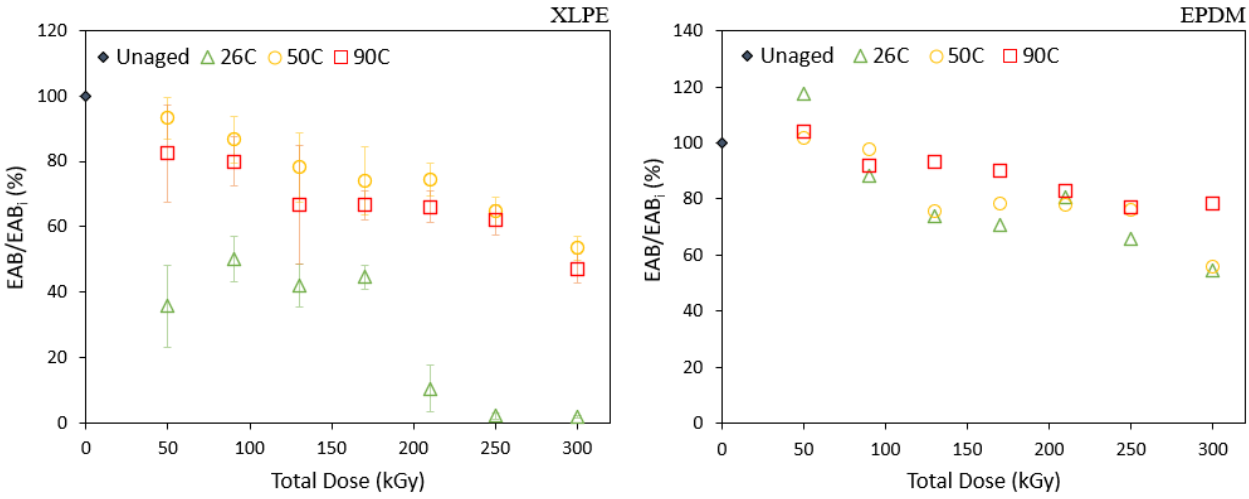

Figure 3. Average relative elongation at break (EAB/EAB$_i$) of insulation specimens after aging. Error is indicated as one standard deviation. EAB$_i$ is 438.0 ± 29.7 (%) for XLPE, and 305.5 ± 15.1 (%) for EPDM.

6.2 Mass Change

The relative mass change ($\Delta m/m_i$) of the insulation specimens after aging is compared to that of the same specimens before aging in Figure 4. For the investigated XLPE material, two different dominant degradation mechanisms were observed based upon the irradiation temperature. At irradiation temperatures of 26°C and 50°C, mass was observed to increase linearly, potentially due to oxygen addition with the formation of carbonyl groups. On the other hand, mass was observed to linearly decrease at an irradiation temperature of 90°C, hypothetically attributed to chain scission and breakdown of thermally weak species. The reverse was observed in previous work where ITE was reported for an XLPO material (Celina et al., 1998) – chain scission was found to occur at low temperatures, whereas cross-linking was found to occur at high temperature. For EPDM, an initial decrease in mass change for all three temperatures was measured, with a slight increase in mass change accompanied by large uncertainty. Potential ITE were not directly observed with mass change for XLPE or EPDM.

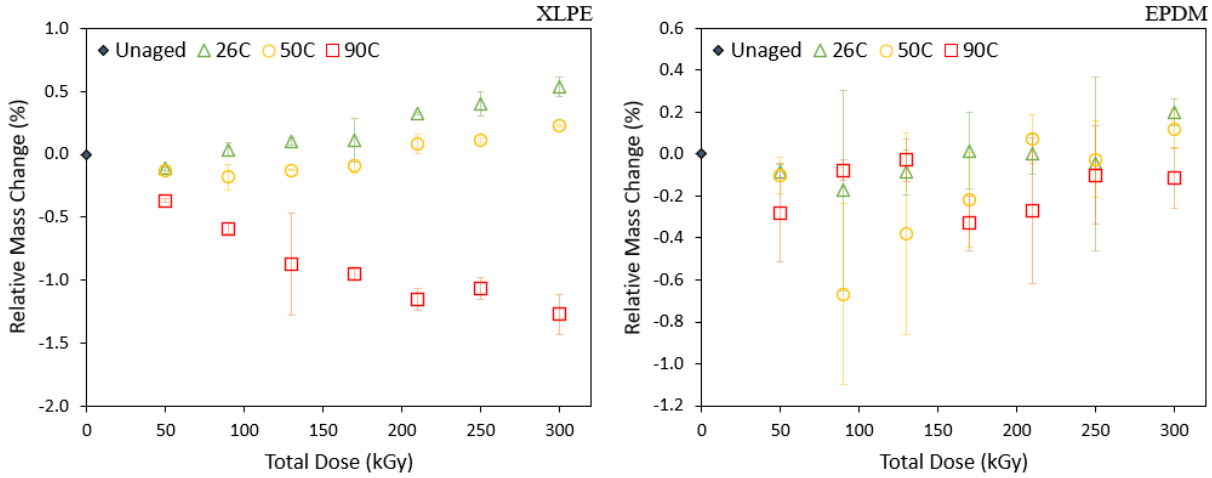

Figure 4. Average relative mass change ($\Delta m/m_i$) of insulation specimens after aging. Error is indicated as one standard deviation.

6.3 Yellowness Index

Yellowness index (YI) of the insulation specimens after aging is compared to that of the unaged insulations specimens in Figure 5. For both material types, increasing yellowing was observed with increasing total absorbed dose, within expectations of previous work (Fuchs et al., 2021). With increasing dose, the increase in YI values were observed to slow down after approximately 170 kGy for XLPE and to plateau for EPDM, similar to previous findings (Spencer et al., 2020). In addition, for both material types, largest increases in YI were observed at the highest aging temperature (90°C), again within expectations (Ni et al., 2021) and potentially indicative of YI being a metric that is not sensitive to ITE.

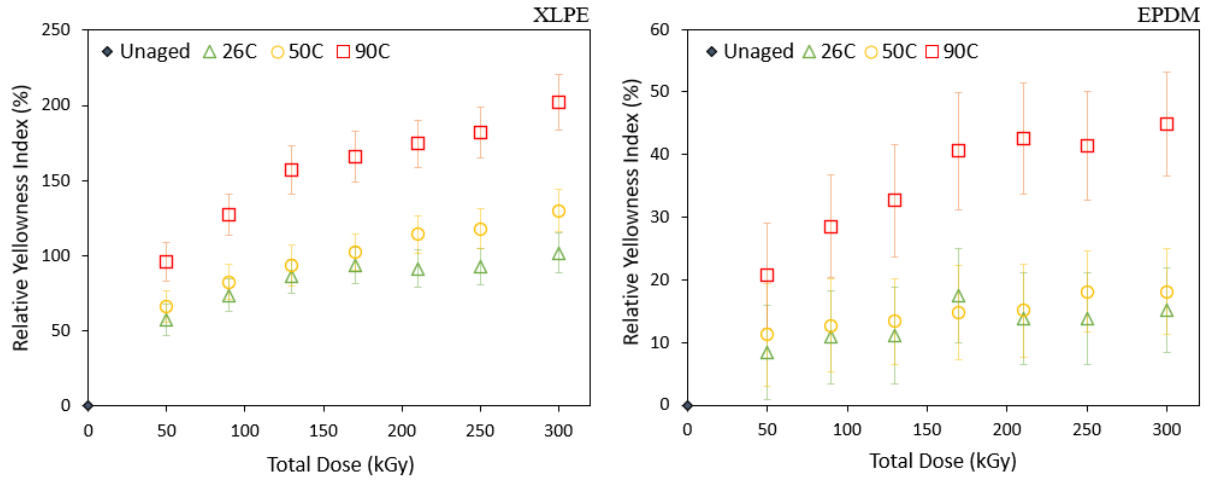

Figure 5. Average relative yellowness index ($\Delta YI/YI_i$) of insulation specimens after aging. Error is indicated as one standard deviation. YI_i is 25.4 ± 1.4 (a.u.) for XLPE, and 39.5 ± 1.9 (a.u.) for EPDM.

6.4 Carbonyl Index

Carbonyl index is a convenient metric for oxidation because carbonyl groups are common oxidation byproducts and methylene groups form a common backbone for both XLPE and EPDM. Measured relative carbonyl index (CI) for both material types are shown in Figure 6. For both material types, an increase in carbonyl index was measured with increasing dose, in agreement with previous work (Li et al., 2021) and an indicator of oxidation within the evaluated materials (Almond et al., 2020). For XLPE, a linear increase in carbonyl index was observed for all three temperatures, with the largest increase occurring for the highest aging temperature (90°C), consistent with observations from YI measurement. On the other hand, EPDM demonstrated plateauing of carbonyl index trends at an absorbed dose of approximately 170 kGy, again similar to that observed with YI; however, at an aging temperature of 90°C, a sudden increase of carbonyl index at the maximum absorbed dose (300 kGy) was found. As no carbonyl index trend demonstrated increased variation at the lowest aging temperature (26°C), it is hypothesized that carbonyl index is not sensitive to ITE for these material types.

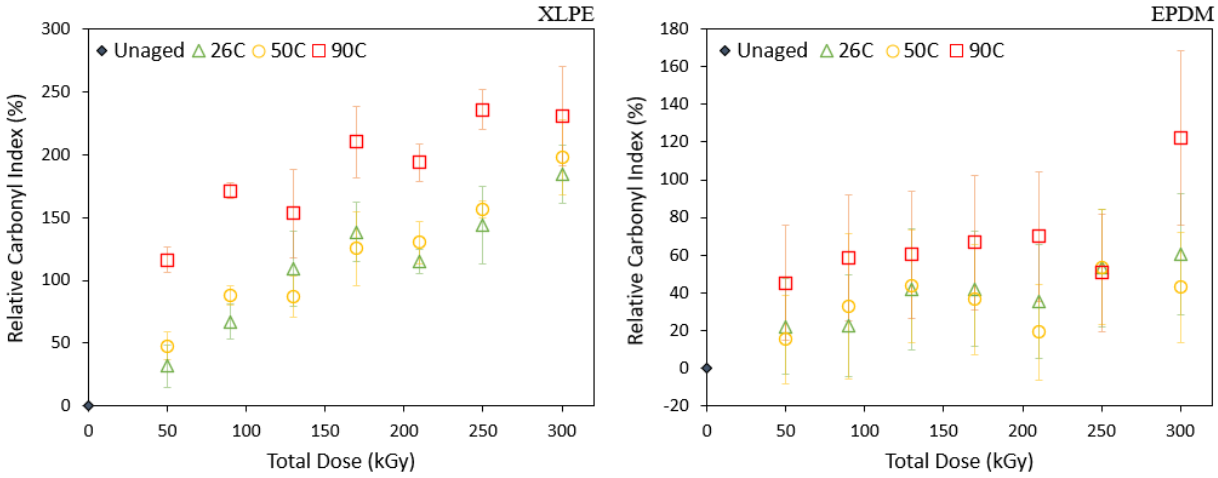

Figure 6. Average relative carbonyl index ($\Delta CI/CI_i$) of insulation specimens after aging. Error is indicated as one standard deviation. CI_i is 0.17 ± 0.002 (a.u.) for XLPE, and 0.18 ± 0.04 (a.u.) for EPDM.

6.5 Density

Density measurement of polymeric materials is important as densification is an indicator of degradation (Subudhi, 1996). Density (ρ) of the insulation specimens after aging is compared to that of the unaged insulations specimens in Figure 7. For both material types, density fluctuated with total absorbed dose, indicating stability at the exposures and dose rate explored. More specifically, density was observed to be approximately equivalent between irradiation temperatures (26°C, 50°C, and 90°C), potentially indicating density is not a sensitive metric to ITE for these material types.

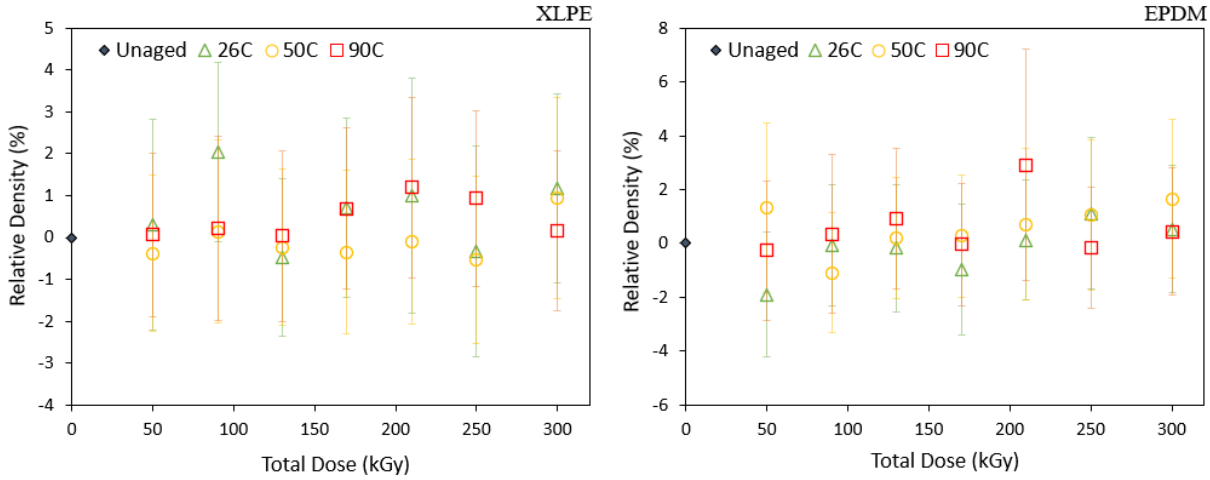

Figure 7. Relative average density ($\Delta\rho/\rho_i$) of insulation specimens after aging. Error is indicated as one standard deviation. ρ_i is 1.29 ± 0.02 (g/cc) for XLPE, and 1.30 ± 0.03 (g/cc) for EPDM.

6.6 Indenter Modulus and Relaxation Constant

The indenter modulus (IM) is useful as a metric to track degradation in polymeric materials as it is an indicator of the compressive stiffness of a material, which has been shown to vary with aging (Fifield et al., 2020). In addition, the relaxation constant (τ) is useful to track the recovery behavior of a deformed polymeric material. IM and τ values of the insulation specimens after aging are compared to those of the unaged insulations specimens in Figure 8 and Figure 9, respectively. For XLPE, an increasing trend for indenter modulus was observed at all irradiation temperatures, with the largest increase found for the highest evaluated temperature (90°C)—within expectations. Furthermore, aging at 50°C produced an indenter modulus response between those produced with aging at 26°C and 90°C; by comparison, YI and CI isotherms at 50°C were closer to those at 26°C. Similarly, the relaxation constant decreased the most at the highest evaluated temperature (90°C) and the least at 26°C. For EPDM, indenter modulus was observed to slightly increase with total absorbed dose, with no obvious difference between the evaluated temperatures. The relaxation constant trend for EPDM was similar to XLPE, with the lowest relaxation constant found for the highest exposure temperature (90°C). Overall, indenter modulus and relaxation constant were not observed to be sensitive to ITE for the investigated materials.

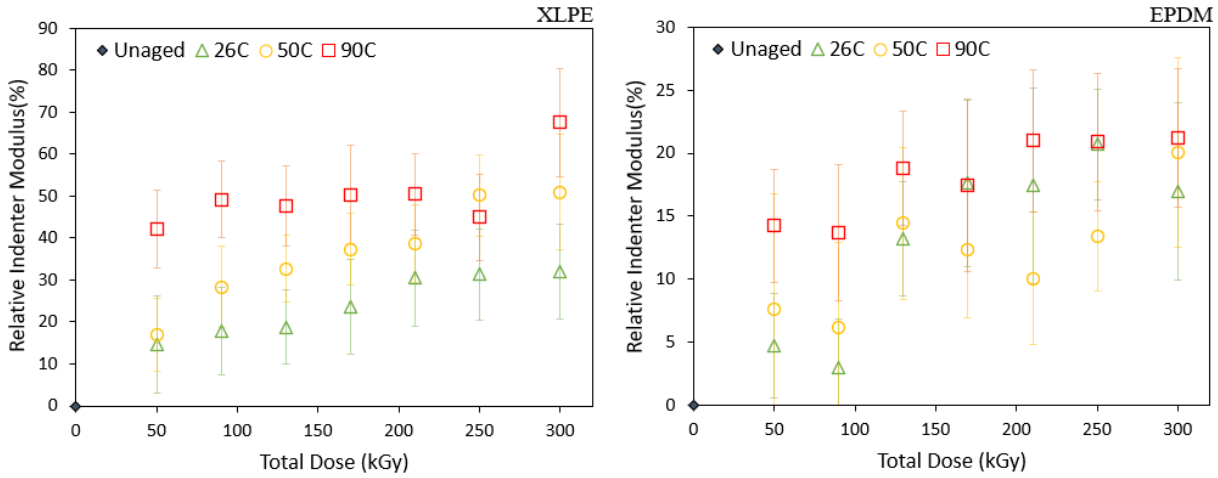

Figure 8. Average relative indenter modulus ($\Delta IM/IM_i$) of insulation specimens after aging. Error is indicated as one standard deviation. IM_i is 32.0 ± 1.8 (N/mm) for XLPE, and 14.6 ± 0.5 (N/mm) for EPDM.

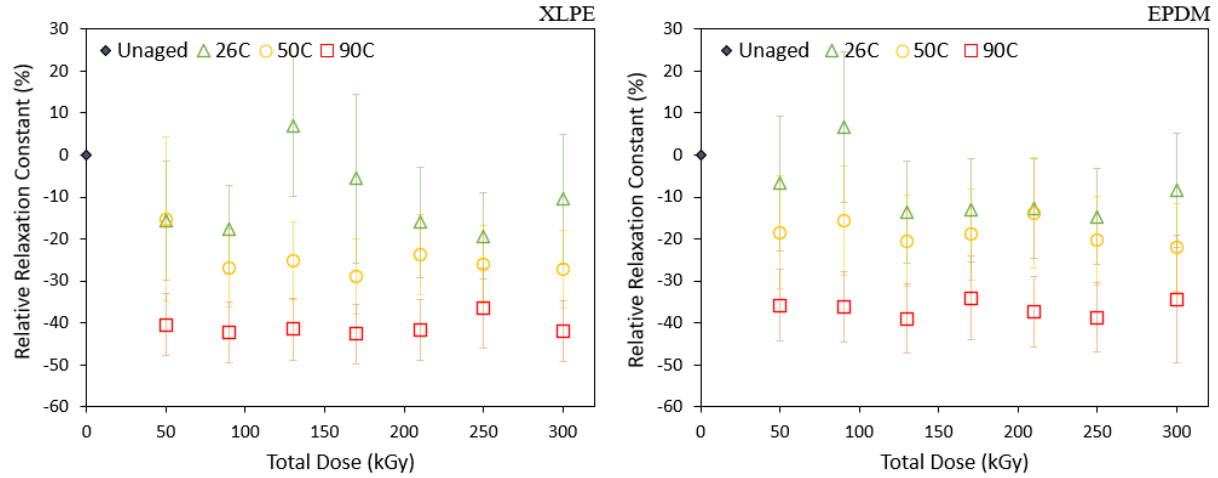

Figure 9. Average relative relaxation time ($\Delta\tau/\tau_i$) of insulation specimens after aging. Error is indicated as one standard deviation. τ_i is 81.9 ± 10.1 (s) for XLPE, and 79.5 ± 10.5 (s) for EPDM.

7. DISCUSSION

Based on the results of the two representative materials studied, ITE were only observed with tensile elongation at break for XLPE. Mechanical properties within the linear elastic deformation range (such as indenter modulus and relaxation time), chemical properties (such as carbonyl index and yellowness index), and mass change of XLPE demonstrated trends as expected; that is, the evaluated materials demonstrated increased degradation at higher temperatures. Density and mass change of EPDM were not sensitive enough to show differences between aging temperatures. Results of this work, including previous work from the literature, are summarized in Table 5. Based upon previous work, density was reported to show ITE for a cross-linked polyolefin (XLPO) (Celina et al., 1996), but not for all materials investigated (Celina et al., 1998). On the other hand, it's been observed that low gel content was correlated with anomalously low durability, indicating chain scission is likely the predominant mechanism during ITE. In addition, it has been observed that ITE have effectively vanished in certain materials with annealing at 140°C (Celina et al., 1998), leading to the recovery of properties such as mechanical strength and increase in gel content.

Table 5. Summary of test metrics influenced by ITE.

Test Metric	Observed ITE
Tensile elongation	Brittle failure that's earlier than expected [(Celina et al., 1998, 1996), this work]
O_2 consumption	No ITE (Celina et al., 1996)
Gel content	Lower gel content or chain scission dominant (Celina et al., 1998, 1996)
Density	Pronounced increase (Celina et al., 1996) or no ITE [(Celina et al., 1998), this work]
Mass change	No ITE [this work]
Yellowness index	No ITE [this work]
Carbonyl index	No ITE [this work]
Indenter modulus	No ITE [this work]
Relaxation constant	No ITE [this work]

Two hypotheses have been proposed and investigated in literature regarding chain scission correlated ITE and ITE recovery: (i) metastable residual radicals at low temperature such as peroxides could re-initiate crosslinking at high temperatures and (ii) partial melting of the crystalline phase around 60°C results in higher mobility that diminishes ITE (Celina et al., 1998). However, in regard to hypothesis (i), no evidence has been found to support residual radical induced crosslinking during annealing, which included searching for intermediate radicals through electron spin resonance (ESR) spectroscopy, investigation of FTIR hydroperoxide bands, and also FTIR emission spectroscopy following NO, SO_2, and PH_3 treatment. On the other hand, hypothesis (ii) conceptually explains the phenomena of ITE through changes in molecular morphology upon early melting of the crystalline structures. In this work, the onset of melting was observed at approximately 80°C as shown in Figure 10, slightly higher than 60°C reported in literature (Celina et al., 1998). Although the keywords in this hypothesis ("mobility" or "morphology") are somewhat vague, the hypothesis is consistent with classic rubber elasticity theory (Rubinstein et al., 2003). While deformation of metals and ceramics requires displacing atoms from their energetic equilibrium position, stretching a polymer chain increases its end-to-end distance ($\vec{R}$) and results in fewer possible arrangements, i.e., lower conformational entropy (S). This "entropic spring" model explains elastic behaviors of polymers, especially rubbers. According to Flory construction, more than 90% of the total force in the rubbery state comes from the entropic component and the rest from the energetic component. For an ideal linear chain consisting of N Kuhn segments of length b, entropy (S) is the Boltzmann constant (k) times the number of states (Ω), as given in Equation (6). (Rubinstein et al., 2003; Flory, 1953)

$$S\left(N, \vec{R}\right) = k ln\, \Omega\left(N, \vec{R}\right) \tag{6}$$

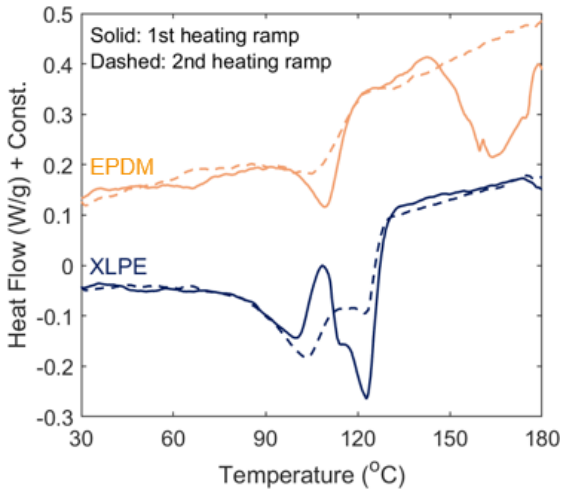

Figure 10. Differential scanning calorimetry measurement on the as-received materials.

For semi-crystalline polymers subjected to low-temperature irradiation-combined aging, chains in the amorphous phase are restricted in a confined region and chain scission is favored. The number of Kuhn segments in a chain (N) decreases during chain scission, which significantly reduces entropy and allows little deformation in subsequent mechanical testing. Since the broken chain ends are connected to folded chains in the crystalline phase, upon annealing above the melting temperature the entire chain can rearrange and re-crystalize, equivalent to an increase in N and S and recovery of mechanical durability. If polymers are irradiated at high temperatures, rearrangement of chains in the amorphous and crystalline regions can occur during aging and avoid chain scission in the amorphous region. To further test if this assumption is true, quantification of the entropy changes before and after irradiation through experiments or simulation is needed.

To support discussion regarding potential ITE applied to historical cable qualification, tensile elongation at break for insulation specimens undergoing synergistic exposures (Fifield et al., 2020) are shown in Figure 11. This work observed irradiation at a dose rate of 300 Gy/hr at ambient (26°C), followed by annealing at 150°C with no irradiation (R+T) to produce reduced degradation compared to the reverse exposure sequence (T+R) or the combined exposure(T/R) for XLPE-2 (here, RSCC I46-0021), in-line with the above discussion regarding ITE and further supporting the finding that XLPE is a material that is sensitive to ITE. Conversely, Figure 11 demonstrates reduced degradation for EPDM (same material as in this report) undergoing the T+R aging scenario, also potentially indicative of EPDM not being a material that is sensitive to ITE. In terms of historical cable qualification, the T+R aging scenario was the predominant aging scenario used by cable manufacturers during qualification (Subudhi, 1996), which may indicate conservatism in historical cable qualification towards ITE, particularly for XLPE cable insulation.

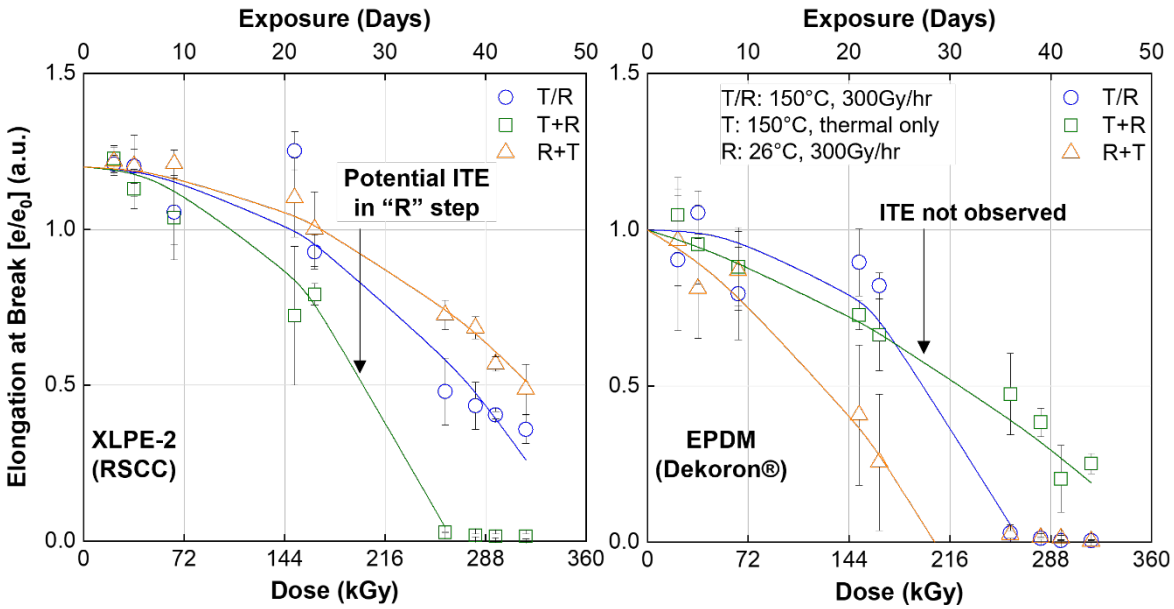

Figure 11. Synergistic response of cable insulation specimens at constant dose rate (Fifield et al., 2020). The averaged relative elongation at break is shown for the aged (left) XLPE-2 and (right) EPDM insulation specimens. The solid lines represent fitting of the data to the model discussed in Fifield et al. The *T+R* condition represents thermal aging at 150°C, followed by irradiation at a dose rate of 300 Gy/hr for the same time period at ambient temperature (26°C).

8. CONCLUSIONS

The objective of this report is to address one of the four cable aging knowledge gaps, inverse temperature effects, emphasized by Fifield et al. (2018). In this work, inverse temperature effects refer to increased degradation of electrical cable insulation at low temperatures, as opposed to high temperatures, during accelerated aging with gamma irradiation. Such inverse temperature effects are a concern as some materials may age faster near service conditions, which would lead to overestimation of lifetime from accelerated aging predictions for those materials.

In this report, nuclear cable insulation specimens of two of the most common types, XPLE and EPDM, from two of the most sourced manufacturers, Brand-Rex and Samuel Moore, were subjected to accelerated aging conditions at temperatures (26°C, 50°C, and 90°C) previously observed to be associated with anomalous property change, or inverse temperature effects. To evaluate the presence of ITE, and the sensitivity of metrics to ITE, six characterization methods were employed (elongation at break, mass change, yellowness index, carbonyl index, density, and indenter modulus). It was observed that,

- ITE was evident in XLPE, while not evident in EPDM;
- ITE was evident in tensile elongation at break (EAB) data;
- ITE was not evident from mass change, yellowness index, carbonyl index, density, indenter modulus, and relaxation constant.

Significantly more rapid degradation at 26°C than at 50°C or 90°C for XLPE elongation at break is of potential concern if qualification lifetime is based on extrapolated performance from higher temperature aging as service aging occurs close to 26°C; however, the predominate aging scenario during historical cable qualification was thermal aging followed by irradiation at ambient, which may imply ITE susceptible cable insulation underwent the most conservative aging condition. None of the other chemical or physical property measurements of XLPE or EPDM exhibited this anomalous temperature effect observed with

EAB. ITE was not observed in EPDM elongation at break data and insulation values remained above threshold at all temperatures up to the maximum dose explored. The effects of gamma aging at various temperatures on additional material properties such as thermal phase transitions and dielectric breakdown voltage would be of interest for increased understanding of the mechanisms of ITE and their implications for insulation functional performance.

The results in this report do not support the conclusion that ITE in cable qualification necessarily exclude safe continued use of existing cables. Inverse temperature effects were found to differ based on insulation material and on property measured. The practice of subjecting cables to thermal aging followed by radiation aging at room temperature in qualification appears to be a conservative scenario for materials exhibiting ITE. Ongoing non-destructive cable system condition monitoring is encouraged to support repair and replace decisions for continued safe and effective use of electrical cables in long term operation.

9. REFERENCES

Almond, J., Sugumaar, P., Wenzel, M.N., Hill, G., Wallis, C., 2020. *Determination of the carbonyl index of polyethylene and polypropylene using specified area under band methodology with ATR-FTIR spectroscopy*. e-Polymers 20, 369–381. https://doi.org/10.1515/epoly-2020-0041.

Beleites, C., Sergo, V., 2013. *hyperSpec: a package to handle hyperspectral data sets in R*.

Burns, S.A., 2017. *Generating Reflectance Curves from sRGB Triplets*, 1–39.

Celina, M., Gillen, K.T., Clough, R.L., 1998. *Inverse temperature and annealing phenomena during degradation of crosslinked polyolefins*. Polym. Degrad. Stab. 61, 231–244. https://doi.org/10.1016/S0141-3910(97)00142-0.

Celina, M., Gillen, K.T., Wise, J., Clough, R.L., 1996. *Anomalous aging phenomena in a crosslinked polyolefin cable insulation*. Radiat. Phys. Chem. 48, 613–626. https://doi.org/10.1016/0969-806X(96)00083-7.

EIA. 2022. "U.S. energy facts explained." U.S. Energy Information Administration. Last modified June 10, 2022. Accessed September 9, 2022. https://www.eia.gov/energyexplained/us-energy-facts/

Fifield, L.S., 2016, *Status Report and Research Plan for Cables Harvested from Crystal River Unit 3 Nuclear Generating Plant*, PNNL-25833, Richland, WA.

Fifield, L.S., Huang, Q., Childers, M.I., Zwoster, A.J., 2016, *Progress in Characterizing Naturally-Aged Nuclear Power Plant Cables*, PNNL-25439, Richland, WA.

Fifield, L.S., Spencer, M.P., Ni, Y., Li, D., Pallaka, M.R., Bisel, T.T., Zwoster, A., Murphy, M.K., 2020. *Sequential Versus Simultaneous Aging of XLPE and EPDM Nuclear Cable Insulation Subjected to Elevated Temperature and Gamma Radiation (Final Results)*, PNNL-30041 Rev. 1. Richland, WA.

Fifield, L.S., Zwoster, A., Murphy, M., 2018. *Initiation of Experimental Campaign to Address Knowledge Gaps Related to Simultaneous Thermal and Gamma Radiation Aging of Crosslinked Polyethylene and Ethylene-Propylene Rubber Cable Insulation*, PNNL-27987. Richland, WA.

Flory, P.J., 1953. *Principals of Polymer Chemistry*. Cornell University Press.

Fuchs, W.K., Spencer, M.P., Li, D., Ni, Y., Zwoster, A., Fifield, L.S., 2021. C*orrelation of Diffusion Limited Oxidation to Color Difference in Accelerated Aging of Electrical Cable Insulation*, in: 2021 IEEE Conference on Electrical Insulation and Dielectric Phenomena (CEIDP). IEEE, pp. 639–642. https://doi.org/10.1109/CEIDP50766.2021.9705346.

Gazdzinski, R.F., Denny, W.M., Toman, G.J., Butwin, R.T., 2000. A*ging Managment Guideline for Commercial Nuclear Power Plants - Electrical Cble and Terminations*, SAND96-0344.

Gillen, K.T., 2019. *Importance of Synergism for Degradation of Elastomers in Combined Radiation Plus Temperature Environments*. Rubber Chem. Technol. 93, 121–141. https://doi.org/10.5254/rct.19.80457.

Gillen, K.T., Clough, R.L., 1992. *Rigorous experimental confirmation of a theoretical model for diffusion-limited oxidation*. Polymer (Guildf). 33, 4358–4365. https://doi.org/10.1016/0032-3861(92)90280-A.

Gillen, K.T., Clough, R.L., 1989. *Time-temperature-dose rate superposition: A methodology for extrapolating accelerated radiation aging data to low dose rate conditions*. Polym. Degrad. Stab. 24, 137–168. https://doi.org/10.1016/0141-3910(89)90108-0.

Gryn'ova, G., Hodgson, J.L., Coote, M.L., 2011. *Revising the mechanism of polymer autooxidation*. Org. Biomol. Chem. 9, 480–490. https://doi.org/10.1039/c0ob00596g.

Li, D., Spencer, M., Pallaka, M.R., Bisel, T.T., Ni, Y., Zwoster, A., Murphy, M.K., Fifield, L.S., 2021. *Principal Component Analysis of Nuclear Cable Insulation Subjected to Elevated Temperature and Gamma Radiation*, in: 2021 IEEE Electrical Insulation Conference (EIC). IEEE, pp. 185–188. https://doi.org/10.1109/EIC49891.2021.9612244.

Ni, Y., Bisel, T.T., Spencer, M.P., Fuchs, W.K., Reddy Pallaka, M., Fifield, L.S., 2021. *Color Change During Thermal Degradation of Polyolefin Electric Cable Insulations*, in: 2021 IEEE Conference on Electrical Insulation and Dielectric Phenomena (CEIDP). IEEE, pp. 129–132. https://doi.org/10.1109/CEIDP50766.2021.9705427.

NRC, 2014. *Expanded Materials Degradation Assessment (EMDA), Volume 5: Aging of Cables and Cable Systems*, Nuclear Regulatory Commission, NUREG/CR-7153.

Simmons, K.L., Ramuhali, P., Brenchley, D.L., Coble, J.B., Hashemian, H.M., Konnick, R., and Ray, S., 2012. *Light Water Reactor Sustainability (LWRS) Program–Non-Destructive Evaluation (NDE) R&D Roadmap for Determining Remaining Useful Life of Aging Cables in Nuclear Power Plants*. PNNL-21731.

Przybytniak, G., Boguski, J., Placek, V., Verardi, L., Fabiani, D., Linde, E., Gedde, U.W., 2015. *Inverse effect in simultaneous thermal and radiation aging of EVA insulation*. Express Polym. Lett. 9, 384–393. https://doi.org/10.3144/expresspolymlett.2015.36.

Rubinstein, M. and Colby, R.H., 2003. *Polymer Physics*. Oxford University Press.

Seguchi, T., Tamura, K., Kudoh, H., Shimada, A., Sugimoto, M., 2015. *Degradation of cable insulation material by accelerated thermal radiation combined ageing*. IEEE Trans. Dielectr. Electr. Insul. 22, 3197–3206. https://doi.org/10.1109/TDEI.2015.004880.

Seguchi, T., Tamura, K., Ohshima, T., Shimada, A., Kudoh, H., 2011. *Degradation mechanisms of cable insulation materials during radiation-thermal ageing in radiation environment*. Radiat. Phys. Chem. 80, 268–273. https://doi.org/10.1016/j.radphyschem.2010.07.045.

Spencer, M.P., Zwoster, A., Bisel, T.T., Murphy, M.K., Fifield, L.S., 2020. *Sequential versus Simultaneous Aging of XLPE Nuclear Cable Insulation Subjected to Elevated Temperature and Gamma Radiation*, in: IEEE Electrical Insulation Conference (EIC). Knoxville, TN, USA.

Subudhi, M., 1996. *Literature Review of Environmental Qualification of Safety-Related Electric Cable*, NUREG/CR-6384.

Troscianko, J., 2020. *Empirical Imaging*. http://www.empiricalimaging.com (accessed 1.23.20).

Troscianko, J., Stevens, M., 2015. *Image calibration and analysis toolbox - a free software suite for objectively measuring reflectance, colour and pattern*. Methods Ecol. Evol. 6, 1320–1331. https://doi.org/10.1111/2041-210X.12439.

Zhang, Y., Wu, Z., Qian, C., Tan, X., Yang, J., Zhong, L., 2020. *Research on lifespan prediction of cross-linked polyethylene material for XLPE cables*. Appl. Sci. 10. https://doi.org/10.3390/APP10155381.